

Article

# Tonalite-Dominated Magmatism in the Abitibi Subprovince, Canada, and Significance for Cu-Au Magmatic-Hydrothermal Systems

Lucie Mathieu <sup>1,\*</sup> , Alexandre Crépon <sup>1</sup> and Daniel J. Kontak <sup>2</sup>

<sup>1</sup> Centre D'études sur les Ressources Minérales (CERM), Département des Sciences Appliquées, Université du Québec à Chicoutimi (UQAC), 555 blvd. de l'université, Chicoutimi, QC G7H 2B1, Canada; alexandre.crepon1@uqac.ca

<sup>2</sup> Mineral Exploration Research Centre, Harquail School of Earth Sciences, Goodman School of Mines, Laurentian University, 935 Ramsey Lake Road, Sudbury, ON P3E 2C6, Canada; dkontak@laurentian.ca

\* Correspondence: lucie1.mathieu@uqac.ca; Tel.: +1-418-545-5011 (ext. 2538)

Received: 8 February 2020; Accepted: 3 March 2020; Published: 7 March 2020



**Abstract:** In Archean greenstone belts, magmatism is dominated by intrusive and volcanic rocks with tholeiitic affinities, as well as tonalite- and granodiorite-dominated large-volume batholiths, i.e., tonalite–trondhjemite–granodiorite (TTG) suites. These intrusions are associated with poorly documented mineralization (Cu-Au porphyries) that, in the Neoproterozoic Abitibi Subprovince (>2.79 to ~2.65 Ga), Superior Province, Canada, are associated with diorite bearing plutons, i.e., tonalite–trondhjemite–diorite (TTD) suites. The importance of TTG versus TTD suites in the evolution of greenstone belts and of their magmatic-hydrothermal systems and related mineralization is unconstrained. The aim of this study was to portray the chemistry and distribution of these suites in the Abitibi Subprovince. The study used data compiled by the geological surveys of Québec and Ontario to evaluate the chemistry of TTG and TTD suites and uncovered two coeval magmas that significantly differentiated (fractional crystallization mostly): 1) a heavy rare earth elements (HREE)-depleted tonalitic magma from high pressure melting of an hydrated basalt source; and 2) a hybrid HREE-undepleted magma that may be a mixture of mantle-derived (tholeiite) and tonalitic melts. The HREE-depleted rocks (mostly tonalite and granodiorite) display chemical characteristics of TTG suites (HREE, Ti, Nb, Ta, Y, and Sr depletion, lack of mafic unit, Na-rich), while the other rocks (tonalite and diorite) formed TTD suites. Tonalite-dominated magmatism, in the Abitibi Subprovince, comprises crustal melts as well as a significant proportion of mantle-derived magmas and this may be essential for Cu-Au magmatic-hydrothermal mineralizing systems.

**Keywords:** tonalite; granodiorite; diorite; TTG suite; TTD suite; magmatic-hydrothermal systems; Archean magmatism; greenstone belt; Abitibi Subprovince; Cu-Au mineralization

## 1. Introduction

The Abitibi Subprovince is the largest continuous greenstone belt of the Canadian Shield (Figure 1) [1]. In greenstone belts, the main magmatic phase produced magmas with tholeiitic affinities (mafic lava flows and layered intrusions), as well as tonalite- and granodiorite-dominated large-volume batholiths [2–4]. In the Abitibi Subprovince, an additional rock type (diorite) is observed as part of tonalite plutons associated with Cu-Au magmatic-hydrothermal systems [5,6]. The petrogenetic evolution, as well as the geodynamic and economic significance of the tonalite, granodiorite, and diorite suite, is not fully resolved [4]. The aim of this study is therefore twofold: 1) to examine the chemistry and distribution of these intrusive rocks in greenstone belts, using the Abitibi Subprovince

as an example; and 2) to address the potential metallogenic relevance of these petrologically different suites, which may have implications on a much larger scale.

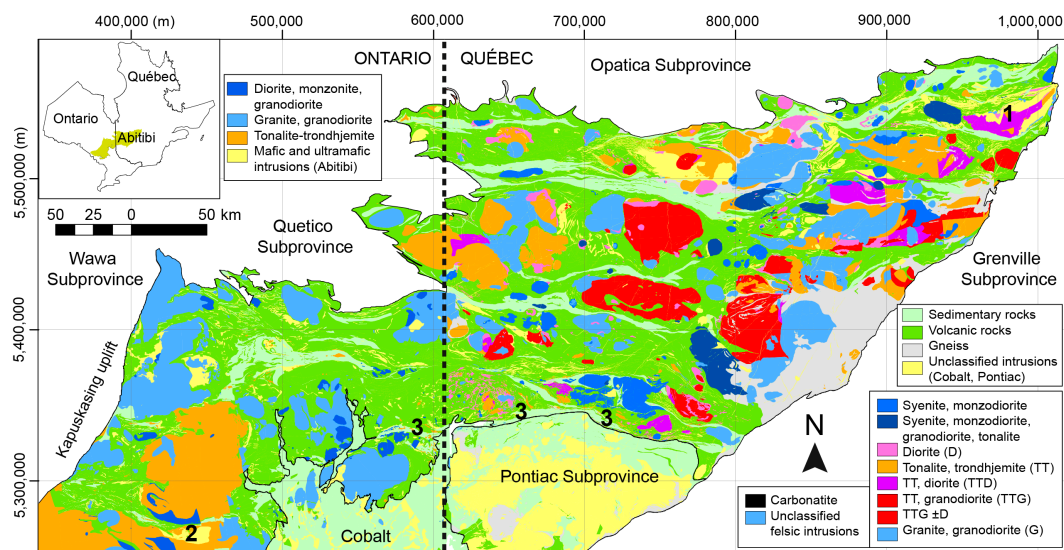


**Figure 1.** Geological map of the Abitibi Subprovince showing the distribution of the main lithologies as classified for the need of this study (see text for details). The map is modified from the Ministère de l'Énergie et des Ressources Naturelles de Québec (MERN), Sigeom dataset, and the Ontario Geological Survey (OGS). The projection is UTM NAD83 Zone 17N. Numbers locate the Chibougamau (1) and Chester (2) plutons, as well as the gold-endowed Cadillac-Larder Lake fault zone (3).

The evolution of greenstone belts can be summarized in two main periods. The main magmatic phase is the synvolcanic period, and it is followed by the syntectonic period, i.e., the main sedimentation (e.g., Timiskaming basin in the Abitibi Subprovince) and deformation phase (mostly shortening related to terrane assembly) that leads to cratonization. In the Abitibi Subprovince, the synvolcanic period extends from >2790 to ~2710 Ma (north) and 2730 to 2695 Ma (south), and the syntectonic period extends from 2701 to 2690 Ma (north) and 2695 to 2650 Ma (south) [2,7,8]. The Abitibi Subprovince is renowned for its gold and base-metal mineralization, which are mostly VMS (volcanogenic massive sulfide; synvolcanic period), as well as orogenic and intrusion-related gold (IRG) systems (syntectonic period) that are particularly abundant in the southern part of the subprovince, along the Cadillac-Larder Lake fault zone (Figure 1). Less recognized mineralization corresponds to magmatic-hydrothermal systems related to intermediate-felsic intrusions of the synvolcanic period. These systems are considered as porphyry-style mineralization, and examples include the Central Camp Cu-Au and the Côté-Gold Au-(Cu) deposits associated, respectively, with the Chibougamau pluton and the Chester intrusive complex [5,6] (Figure 1). In greenstone belts, granitoid intrusions of the synvolcanic period are mostly tonalite–trondhjemite–granodiorite (TTG) suites [9,10], which are felsic (>64 wt% SiO<sub>2</sub>), aluminous (>14–16 wt% Al<sub>2</sub>O<sub>3</sub> for 70 wt% SiO<sub>2</sub>), and Fe-Mg-poor ([Fe<sub>2</sub>O<sub>3T</sub> + MgO + MnO + TiO<sub>2</sub>] < 5 wt%) intrusive rocks characterized by a low K<sub>2</sub>O/Na<sub>2</sub>O ratio (<0.6) [10]. Most TTG suites are also HREE-depleted which reflects their derivation from high-pressure partial melting of mafic crust—i.e., garnet amphibolite [10]. However, the Chibougamau and Chester intrusive complexes are too mafic to be classified as TTG suites, as they contain significant amounts of diorite, and thus, are referred to as tonalite–trondhjemite–diorite (TTD) suites [5,6].

The Central Camp Cu-Au and Côté-Gold Au-(Cu) mineralization raise the question of the importance of TTG versus TTD suites in the evolution of greenstone belts and their magmatic-hydrothermal systems and related mineralization. This contribution uses the Abitibi Subprovince as an example to discuss the chemistry of tonalite-dominated magmatism in the context of greenstone belts. The relative abundance and distribution of diorite, tonalite, and granodiorite are also evaluated, and the importance of these parameters for the prospectivity of

fertile magmatic-hydrothermal systems is discussed. These questions are addressed using whole-rock chemistry and maps provided by Canadian geological surveys.

## 2. Materials and Methods

This study relied on the mapping, U-Pb geochronological data, and whole-rock chemical analyses performed and compiled by the Ministère de l'Énergie et des Ressources Naturelles of Québec (MERN). These data are compiled in the Sigeom dataset, which can be downloaded online free of charge [11]. The dataset covers the Québec half of the Abitibi Subprovince. For Ontario, this study relied on mapping and U-Pb geochronological data performed and compiled by the Ontario Geological Survey (OGS) and the Metal Earth project, and these data can also be downloaded online free of charge [12]. Chemical data for Ontario was performed and compiled by Beakhouse [13].

Maps from the OGS and MERN were combined and displayed using the ArcGIS 10.7 software (Esri, Redlands, CA, USA) (Figures 1 and 2). Maps showing the distribution of lithologies in individual plutons are provided as supplementary material to this contribution. Supplementary material also includes whole-rock chemistry displayed on arachnid and major elements diagrams.

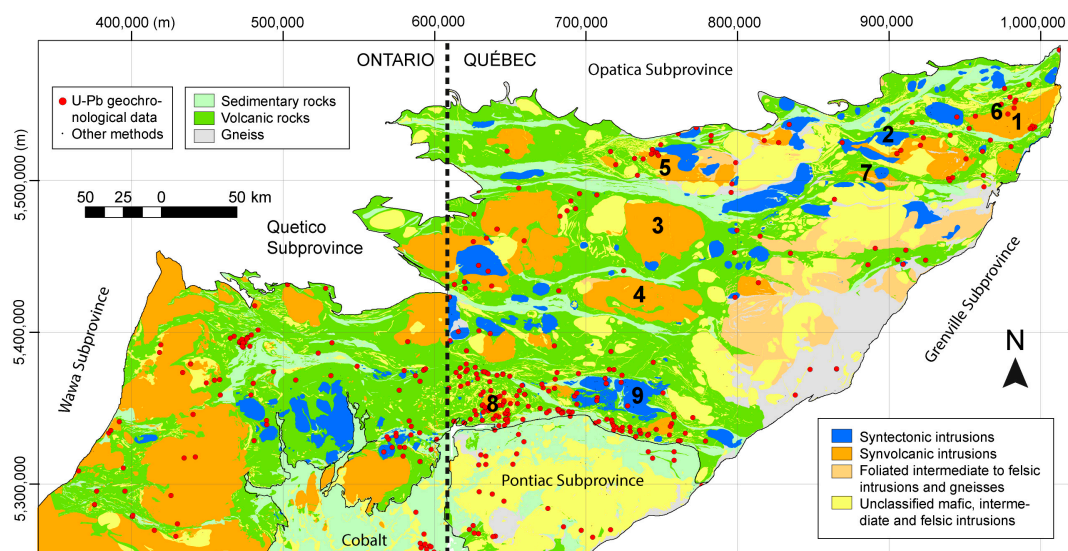


**Figure 2.** Geological map of the Abitibi Subprovince displaying intrusions of the synvolcanic and syntectonic periods. The map is modified from the MERN and OGS dataset, and the projection is UTM NAD83 Zone 17N. Numbers locate the Chibougamau pluton (1), the Ouest granodiorite (2), the Marest (3) and Bernetz (4) batholiths, the Rivière Bell (5), Lac Doré Complex (6), and Opawica River (7) layered intrusions, as well as the Powell, Flavrian and Dufault plutons (8) and the Lacorne pluton (9). In the legend for geochronological data, ‘other methods’ refers to Ar/Ar, K/Ar, Sm/Nd, Pb/Pb, and Rb/Sr data (cooling ages, age of peak metamorphism, etc.).

Whole-rock chemical data of the Sigeom dataset were performed on behalf of the MERN by Activation Laboratories Ltd. (Actlabs, Ancaster, Ontario, Canada). Samples were decomposed by lithium metaborate or tetraborate fusion and were analyzed by inductively coupled plasma (ICP)-optical emission spectroscopy (OES) and ICP-mass spectrometry (MS) for major and trace elements, respectively. The detection limits are 0.01 wt% for major elements and 0.1–1 ppm for trace elements. Other analyses were performed on behalf of mining companies and universities as part of exploration and research programs. For this study, only samples of intrusive rocks with major and rare earth elements (REE) analyzed were considered. Iron and volatiles were reported as  $\text{Fe}_2\text{O}_{3T}$  and LOI, respectively, and FeO,  $\text{Fe}_2\text{O}_3$ ,  $\text{H}_2\text{O}$ ,  $\text{CO}_2$ , and S values were available for <10% of the analyses. When unavailable,  $\text{Fe}_2\text{O}_{3T}$  and LOI were calculated using reported iron ( $\text{FeO} \cdot 1.1113 + \text{Fe}_2\text{O}_3$ ) and volatile ( $\text{H}_2\text{O} + \text{CO}_2 + \text{S}$ ) values. From this, totals were calculated, and only data for which the

total was between 90 and 110 wt% were imported into the ArcGIS software ( $n = 5006$  for the Sigeom dataset), as data that did not satisfy this condition were either incomplete or poor quality analyses. Totals  $>100$  wt% are the consequence of iron reported as  $\text{Fe}_2\text{O}_3\text{T}$  and can be due to GOF (gain on fire) for carbonate and sulfide-bearing rocks, while totals  $<100$  wt% correspond to partial analyses (e.g., unreported volatiles values). However, these analyses were considered to maintain analytical coverage for the studied greenstone belt. Among these, only samples collected from the intermediate-felsic intrusive rocks displayed in Figure 1 are considered ( $n = 840$ ). For Ontario, only samples identified as diorite, granodiorite, tonalite, as well as intermediate-felsic intrusions of the synvolcanic period, were considered ( $n = 201$  for the Beakhouse dataset [13]).

### 3. Spatial Distribution of Intrusive Rocks

#### 3.1. Distribution of the Main Lithologies

Most of the intermediate-felsic plutons of the Abitibi Subprovince are multiphase intrusions. Two or more intrusive phases with distinct composition and/or ages can generally be identified at the outcrop scale, e.g., the Chibougamau pluton [6]. At the scale of the Abitibi Subprovince, such areas are mapped as units made of two or more lithologies and the MERN map contains hundreds of unit types. In this study, the units of the Sigeom dataset were re-classified into nine categories of intermediate-felsic intrusive rocks (Figure 1) as listed below.

- Granodiorite-granite (30.5%)—units with granite and/or granodiorite as the main lithology;
- Tonalite-granodiorite (21.7%)—units dominated by tonalite and granodiorite intrusive rocks with similar or distinct ages;
- Tonalite (20.6%)—units dominated by tonalite rocks and locally referred to as leucotonalite, i.e., quartz-rich tonalite and trondhjemite;
- Tonalite-diorite (6.5%)—diorite and tonalite dominated intrusions;
- Diorite (6.2%)—diorite-dominated plutons;
- Tonalite-granodiorite-(diorite) (1.0%)—tonalite- and granodiorite-rich intrusions with minor amounts of diorite;
- Syenite, monzodiorite, carbonatite, among other (8.2%)—intrusions of the syntectonic period that contain more K than the intrusions considered here;
- Syenite, monzodiorite, granodiorite, tonalite (4.9%)—syntectonic intrusions that crosscut tonalite-dominated intrusions of the synvolcanic and syntectonic periods;
- Unclassified (0.4%)—units identified as intermediate-felsic intrusions.

These units cover 40.9% of the aerial surface of the eastern part of the Abitibi Subprovince, which is also made of metamorphosed (greenschist facies mostly) volcanic rocks (36.1%), sedimentary rocks (8.9%), gneisses with undocumented protoliths (8.4%), and mafic to ultramafic intrusions (5.7%). The lithology classification proposed by the Ontario map has also been simplified. The western half of the Abitibi Subprovince contains volcanic rocks (47.6%), sedimentary rocks (7.9%), mafic to ultramafic intrusions (4.5%), as well as tonalite (13.5%), granite-granodiorite (23.7%), and diorite (2.8%) dominated units (Figure 1).

In the Abitibi Subprovince, the main intrusive lithologies are tonalite and granodiorite (Figure 1), while diorite and tonalite-diorite dominated plutons are less abundant. Intermediate-felsic intrusions are mostly tonalite-granodiorite (61%), tonalite (25%), and tonalite-diorite (15%) in the eastern part of the subprovince (Québec), whereas in the west (Ontario), intrusions are dominated by granodiorite (59%), tonalite (34%), and diorite (7%). Most plutons are TTG suites and TTD suites are less abundant.

Intrusive rocks are well distributed in the Abitibi Subprovince and are most abundant along a NNE-SSW corridor near the Grenville Front, a 1.1 Ga orogeny [14], and along the eastern edge of the greenstone belt, next to the Kapuskasing uplift [15] (Figure 1). Large-volume batholiths are also observed in the central part of the greenstone belt. Some intrusive suites are clusters of tonalite and



granodiorite plutons, while others are made of several phases emplaced in a restricted area to form multiphase plutons. Note that intrusive phases emplaced in the same area are not necessarily coeval, e.g., the Chibougamau pluton [6].

### 3.2. Distribution of Synvolcanic Intrusions

In this section, plutons of the Abitibi Subprovince are tentatively classified as either synvolcanic or syntectonic intrusions. Among the lithologies classified in the previous section, rocks identified as ‘syenite, monzodiorite, carbonatite, among others’ likely formed during the syntectonic period (Figure 2) as, in the Abitibi Subprovince, alkaline intrusions intersect the main foliation observed in volcanic rocks, cross-cut Timiskaming and other sedimentary basins formed during the syntectonic periods, and have syntectonic radiogenic ages. Tonalite, granodiorite, and diorite dominated intrusions, on the other hand, mostly formed during the synvolcanic period, but such intrusions may also display syntectonic ages, e.g., the  $2700 \pm 2$  Ma Ouest granodiorite [16] (Figure 2).

The studied intrusions are classified using U-Pb geochronological data (Figure 2). However, this classification has limits as spatially related synvolcanic and syntectonic intrusions are rarely distinguished on maps. For example, the Chibougamau pluton includes several intrusive phases formed at 2718–2715 Ma (synvolcanic period) and 2705–2701 Ma (syntectonic period) [17–20] that are not distinguished on the MERN map. However, as synvolcanic magmatism is more voluminous than syntectonic magmatism, this pluton is classified as synvolcanic (Figure 2). Additional geochronological data and dedicated mapping are necessary to better portray the distribution of synvolcanic and syntectonic magmatism in the Abitibi Subprovince.

In addition to U-Pb geochronological data, plutons that crosscut sedimentary basins constructed during the syntectonic period are classified as syntectonic intrusions. The undated Marest and Bernetz batholiths are considered synvolcanic, given their large volume and tonalitic composition. The three largest anorthosite-dominated layered intrusions with tholeiitic affinities—Rivière Bell, Lac Doré Complex, and Opawica River—are synvolcanic intrusions [21–23]. Foliated rocks and orthogneiss may also correspond to synvolcanic intrusions (Figure 2).

Most synvolcanic intrusions (Figure 2) are large-volume batholiths (~50 km long in map view or larger) (supplementary material 2), but small-volume plutons also formed during this period. For example, the ~10 km in diameter Powell, Flavrian and Dufault plutons emplaced at shallow depth in the Blake River Complex volcano [24]. Syntectonic intrusions are generally small-volume plugs, but can also form larger (20–30 km long) plutons (Figure 2). For simplification, the general designation ‘syntectonic’ is also applied to late- to post-tectonic intrusions such as the S-type granite phase of the Lacorne pluton [25].

## 4. Chemistry

Most of this section relies on MERN whole-rock chemical analyses (i.e., Sigeom dataset). Only analyses performed on intrusive rocks located in plutons previously identified as tonalite, tonalite-diorite, tonalite-granodiorite, or granodiorite were considered in this section ( $n = 840$ ). Most rocks are sub-alkaline (Figure 3a) and calc-alkaline (Figure 3b). Data scattering seen on the total alkali versus silica (TAS) and alkali- $\text{FeO}_T$ -MgO (AFM) diagrams (Figure 3) is likely due to hydrothermal alteration, which does not seem to affect overall the reliability of the data based on the integrity of rock distributions seen in the chemical plots below. Thus, as rocks modified by hydrothermal alteration are much less abundant than fresh rocks (Figure 3), the chemical considerations reported in this section apply to fresh rocks. Moreover, hydrothermal alteration likely modified the chemistry of a limited amount of rocks because magmatic-hydrothermal and other mineralizing systems are uncommon in intermediate-felsic intrusive rocks. Meanwhile, the Sigeom dataset is likely dominated by fresh rocks.

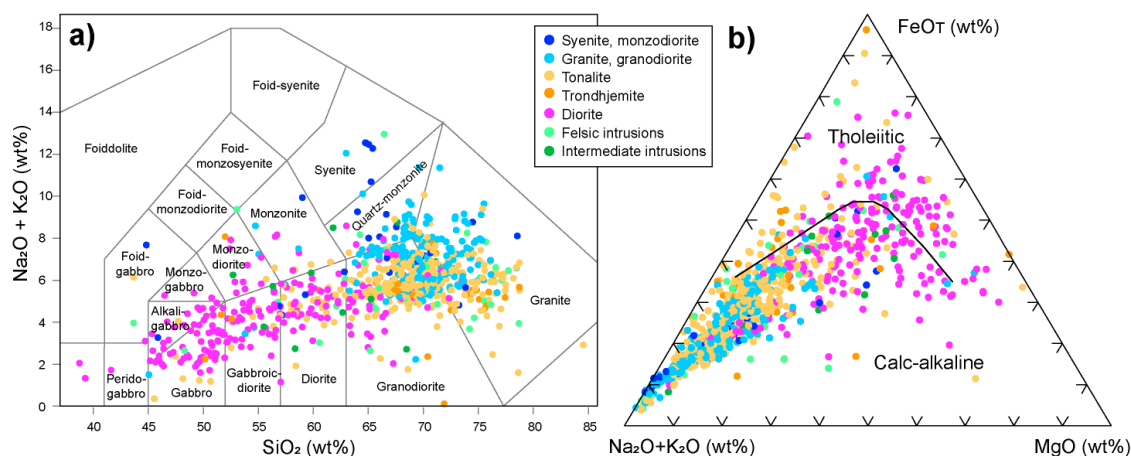


**Figure 3.** Chemical composition of intermediate-felsic intrusive rocks of the Sigeom dataset ( $n = 840$ ) displayed on (a) the total alkali versus silica (TAS) diagram [26] and (b) the alkali- $\text{FeO}_T$ -MgO (AFM) ternary diagram [27]. The rocks identified as felsic and intermediate intrusions are fine-grained and could not be classified precisely in the field.

Analyses were classified using field-based rock names (Figure 4a,b). Most rocks identified as diorite were intermediate to felsic rocks and had the highest Mg number ( $\text{MgO}/[\text{Fe}_2\text{O}_3\text{T} + \text{MgO}]$ ) and Ca contents of the data subset (Figures 3 and 4a,b). A part of the rocks identified as diorite were mafic and may correspond to unrecognized mafic enclaves (Figure 3a). Diorite also displayed the lowest Zr/Ti ratio, which is a proxy for  $\text{SiO}_2$  used to evaluate the extent of magmatic differentiation [28]. The other lithologies were felsic rocks (Figure 3a) with similar Mg numbers, Ca contents, and Zr/Ti ratios (Figure 4a). Trondhjemite and granodiorite are relatively enriched in Na and K compared to tonalite (Figure 4b). There were some inconsistencies between field-based rock names and chemistry, possibly due to imprecise field-estimates of modal proportions (e.g., K-feldspar).

To further evaluate the whole rock chemistry of these suites, samples were classified using the normative quartz–alkali–feldspar–plagioclase (Q-A-P) ternary diagram [29,30]. The normative minerals were calculated using a modified CIPW method to include biotite and amphibole [31] after estimating the values of FeO and  $\text{Fe}_2\text{O}_3$  [32]. The normative minerals were then displayed on the Q-A-P ternary using the method of Le Maitre [32] to distribute normative albite between the A and P poles (Figure 4c). According to this diagram, a significant amount of tonalite and granodiorite are alkaline rocks, which is in disagreement with field observations and the regional context. Considering that albite and anorthite are mostly in plagioclase, normative minerals can be used to approximate the An number of rocks recognized as tonalite (median =  $\text{An}_{24}$ , mean =  $\text{An}_{25}$ ), trondhjemite (median =  $\text{An}_{00}$ , mean =  $\text{An}_{11}$ ), granodiorite (median and mean =  $\text{An}_{21}$ ), and diorite (median and mean =  $\text{An}_{43}$ ) in the field. This is in agreement with known characteristics of TTG suites that mostly contain Na-poor alkali-feldspar and oligoclase [10].

The normative minerals were displayed on the Q-A-P ternary assuming pole A = [normative orthoclase] and pole P = [normative albite + anorthite] (Figure 4d). This is also unrealistic, as alkali-feldspar is not pure orthoclase. However, this classification correlates better with field-based names (Figure 4d) and orthoclase, in the compiled rocks, is likely Na-poor. Diorite classified based on normative quartz and feldspar contents mostly corresponded to rocks identified as diorite in the field (Figure 4d). In contrast, there were discrepancies between classifications for tonalite and granodiorite (Figure 4d), possibly because the modal proportion of the least abundant feldspar (orthoclase) could not be precisely estimated visually in the field and also because CIPW calculations had limitations.

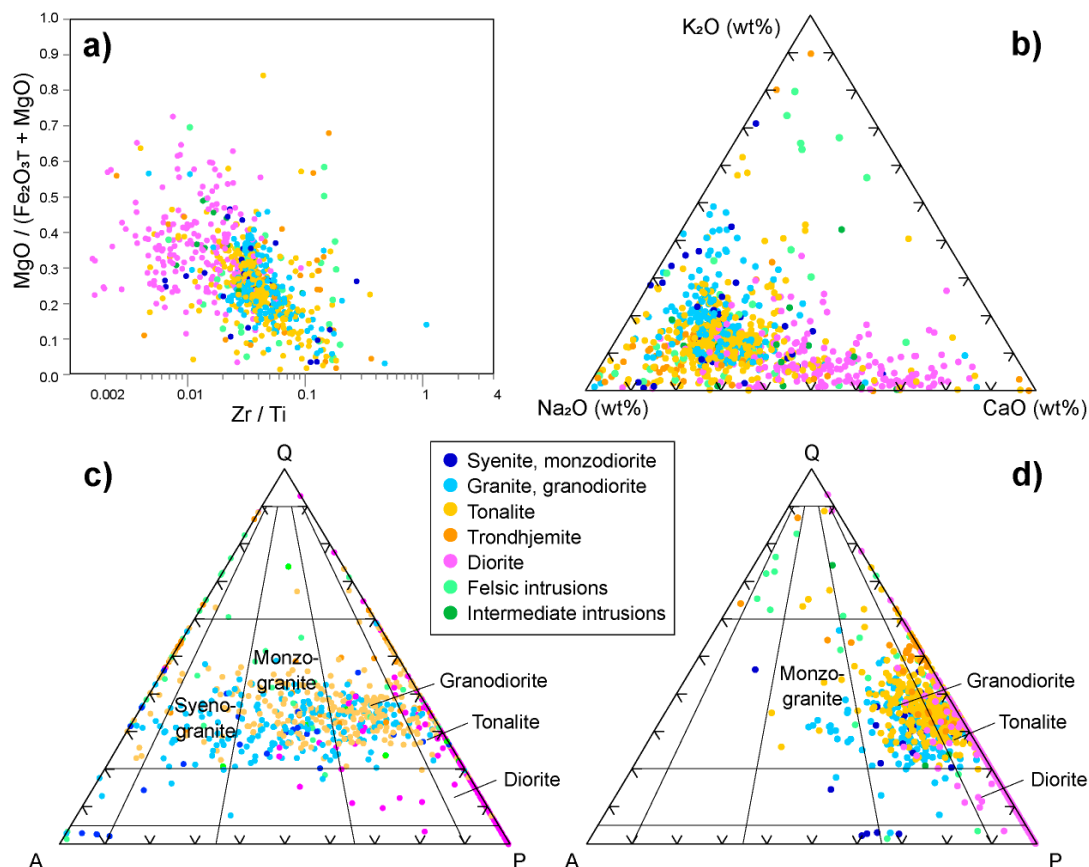


**Figure 4.** Chemical composition of intermediate-felsic intrusive rocks of the Sigeom dataset ( $n = 840$ ) displayed in plots of (a) Mg number vs. Zr/Ti binary, (b)  $Na_2O$ - $K_2O$ - $CaO$  (in wt%) ternary, and (c,d) Q-A-P ternary [29], after performing a CIPW normative calculation [31]. The main difference between (c) and (d) is the method used to distribute normative albite between poles A and P (see text for details). The Le Maître [32] method is used to distribute normative albite between the A and P poles (c). Normative minerals are also displayed assuming pole A = [normative orthoclase] and pole P = [normative albite + anorthite] (d). Color codes correspond to field-based rock types. The rocks identified as felsic and intermediate intrusions are fine-grained and could not be classified precisely in the field.

The rock samples of the Sigeom dataset could also be classified based on their trace element contents. On the REE diagram, rocks display a range of HREE concentrations—where REE profiles are either moderately or strongly fractionated. Rocks are classified based on the  $(La/Yb)_N$  parameter, with La and Yb normalized to primitive mantle [33]. A cut-off value of 6 was used because rocks with  $(La/Yb)_N < 6$  and  $> 6$  displayed distinct chemical characteristics (Figures 5 and 6).

Rocks with  $(La/Yb)_N > 6$  were HREE-depleted (Figure 5a) and resembled typical TTG suites [10]. These rocks had an intermediate Zr/Ti ratio of 0.01 to 0.1 and were Ca depleted (Figure 5c,d). Where ferric and ferrous irons were available ( $n = 22$ ), the  $FeO/(FeO + Fe_2O_3)$  ratio had a median value of 3.7. These rocks also displayed negative Ta-Nb-Ti anomalies (Figure 5b). The Zr and Hf anomalies were negative for samples relatively depleted in  $SiO_2$  and became positive with increasing  $SiO_2$  content. Also, accompanying the increase in  $SiO_2$ ,  $\Sigma REE$  values decreased with  $\Sigma HREE$  decreasing faster than  $\Sigma LREE$ . According to field-based classifications, rocks with  $(La/Yb)_N > 6$  were tonalite and granodiorite, with minor amount of diorite (Table 1).

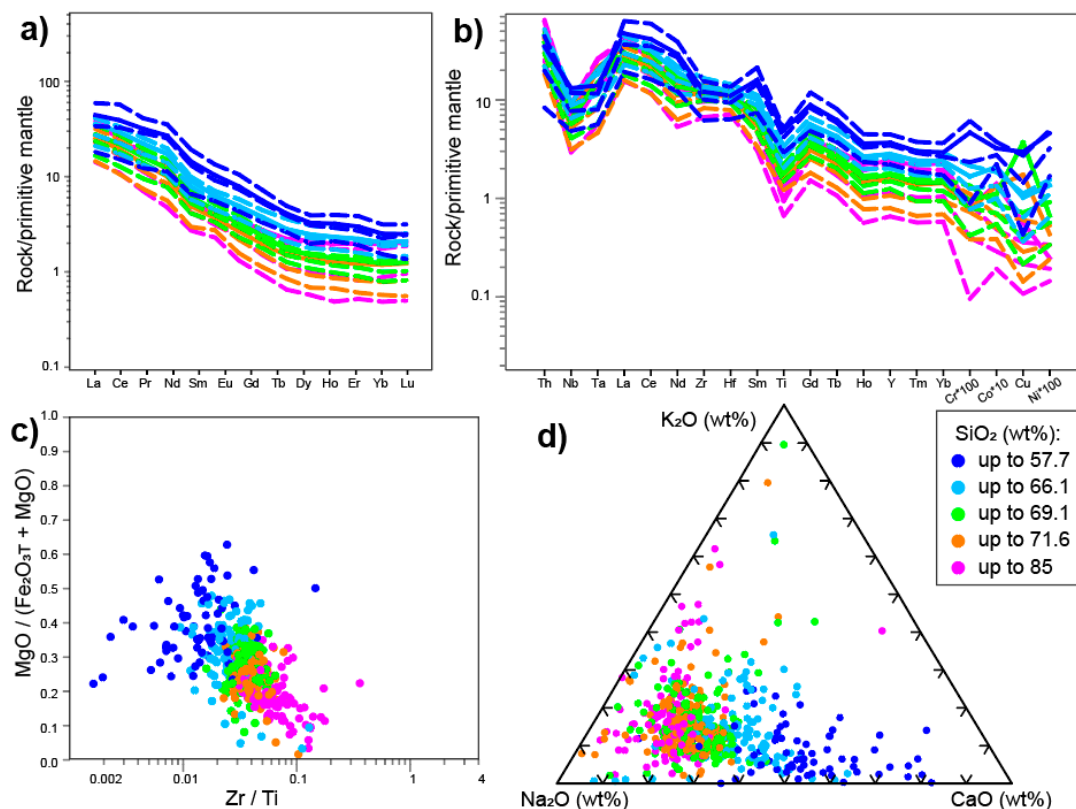


**Figure 5.** Chemical composition of intermediate-felsic intrusive rocks of the Sigeom dataset with  $(La/Yb)_N > 6$  ( $n = 588$ ). Rocks are displayed on (a) a primitive mantle-normalized [34] REE plot, (b) a primitive mantle-normalized [33] multi-element arachnid diagram modified from Pearce [35], (c) a binary plot of Mg number vs Zr/Ti, and (d) a Na<sub>2</sub>O-K<sub>2</sub>O-CaO ternary diagram (in wt%). For plots in (a) and (b), mean values are displayed as solid lines and the 25th, 50th (median) and 75th percentiles are displayed as dashed lines.

**Table 1.** Rock types with fractionated  $((La/Yb)_N > 6)$  and less fractionated  $((La/Yb)_N < 6)$  REE profiles.

	Sigeom Dataset				Beakhouse Dataset	
	$(La/Yb)_N < 6$		$(La/Yb)_N > 6$		$(La/Yb)_N < 6$	$(La/Yb)_N > 6$
	Field <sup>1</sup>	CIPW <sup>2</sup>	Field	CIPW	Field	Field
Granite, granodiorite	8.73 %	11.11%	29.93%	39.29%	30%	35.08%
Diorite	39.29 %	32.14%	17.01%	10.03%	20%	13.61%
Tonalite	32.54 %	45.24%	40.14%	35.37%	40%	27.22%
Trondhjemite	10.32 %		2.55%			
Syenite, monzodiorite	1.59 %		4.93%			
Felsic intrusions	6.75 %		3.57%		10%	9.95%
Intermediate intrusions	0.79 %		1.87%			14.13%
Other		11.15%		15.31%		
n data		252		588	10	191

<sup>1</sup> Rock-type as identified in the field; <sup>2</sup> Rock classified using the Q-A-P ternary [29], after performing a CIPW normative calculation [31].

Rocks with  $(La/Yb)_N < 6$  are less HREE-depleted than rocks with more fractionated REE profiles (Figure 6a), and chemically, they equate to the diorite unit of the Chibougamau pluton [6]. These rocks display a range of Zr/Ti values (0.002 to 0.2) and Ca contents (Figure 6c,d). The FeO/(FeO + Fe<sub>2</sub>O<sub>3</sub>) ratio has a median value of 1.2 ( $n = 40$  samples with ferric and ferrous irons analyzed). Rocks with  $(La/Yb)_N < 6$  display a negative Nb anomaly (Figure 6b). The negative Ti and Eu anomalies were observed in the most SiO<sub>2</sub> enriched rocks only. Moreover,  $\sum REE$  increased with increasing SiO<sub>2</sub> content. According to



field-based classifications, these rocks were diorite and tonalite with minor amounts of granodiorite and trondhjemite (Table 1).

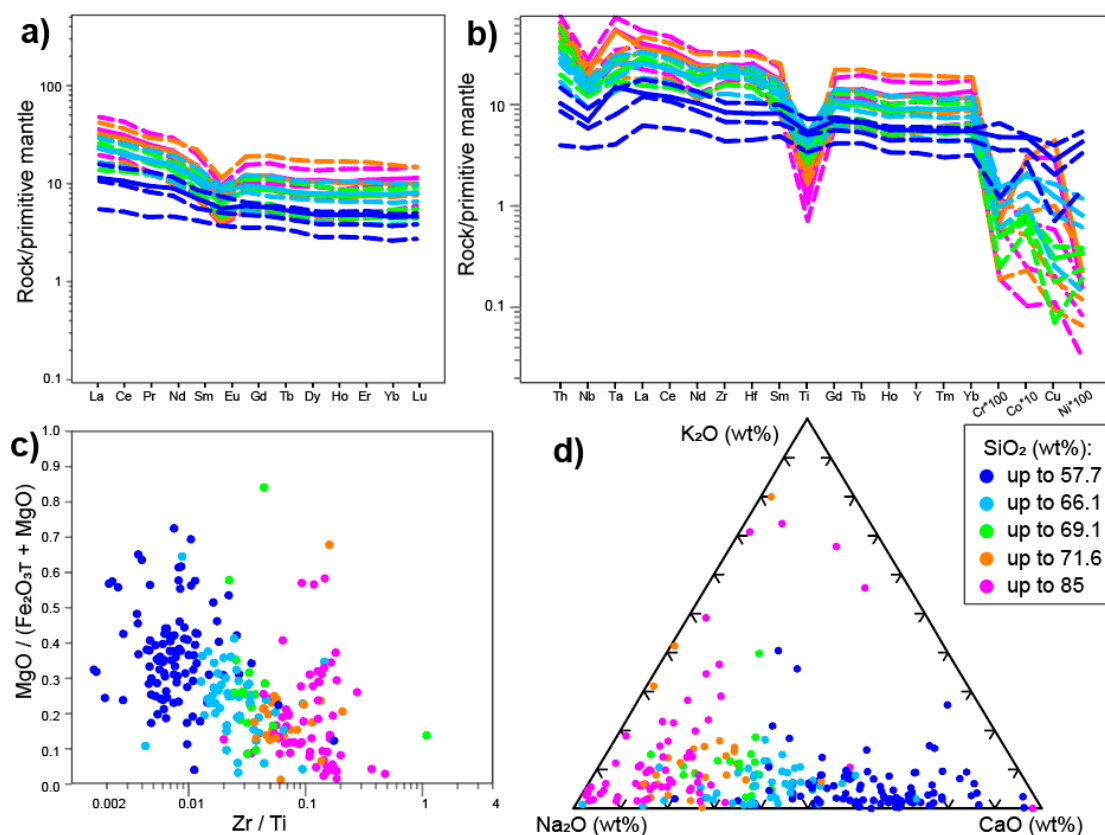


**Figure 6.** Chemical composition of intermediate-felsic intrusive rocks of the Sigeom dataset with  $(La/Yb)_N < 6$  ( $n = 252$ ). Rocks are displayed on (a) a primitive mantle-normalized [33] REE plot, (b) a primitive-mantle normalized [31] multi-element arachnid diagram modified from Pearce [35], (c) a binary plot of Mg number vs. Zr/Ti, and (d) a Na<sub>2</sub>O-K<sub>2</sub>O-CaO (in wt%) ternary diagram. In plots (a) and (b), mean values are displayed as solid lines, and the 25th, 50th (median), and 75th percentiles are displayed as dashed lines.

Concerning the western part of the Abitibi Subprovince, samples compiled by Beakhouse [13] mostly display fractionated REE profiles ( $(La/Yb)_N > 6$ ). They corresponded to tonalite and granodiorite with a minor amount of diorite (Table 1). Samples with  $(La/Yb)_N < 6$  are diorite and tonalite (Table 1). This was consistent with observations made in the eastern part of the subprovince using the Sigeom dataset.

Most plutons are constructed by rocks that are HREE-depleted with  $(La/Yb)_N > 6$  or of both HREE-depleted and HREE-undepleted rocks with any  $(La/Yb)_N$  value (Figure 7). The plutons dominated by HREE-depleted rocks are mostly made of tonalite and granodiorite and are synvolcanic intrusions, except for the Adams, Geikie, and Blackstock plutons that formed at the beginning of the syntectonic period (supplementary material 1). Examples are the Marest and Bernetz batholiths, which span a range of SiO<sub>2</sub> values (52 to 76 wt% SiO<sub>2</sub>, median = 70 wt% SiO<sub>2</sub>), and are made of felsic rocks (tonalite, granodiorite) and a minor amount of intermediate rocks (diorite). Examples of batholiths dominated by HREE-undepleted rocks are synvolcanic diorite and tonalite intrusions, e.g., the Bourlamaque pluton (55 to 65 wt% SiO<sub>2</sub>), as well as tonalite and trondhjemite, e.g., the Flavrian and Powell plutons (52 to 79 wt% SiO<sub>2</sub>, median = 73 wt%).

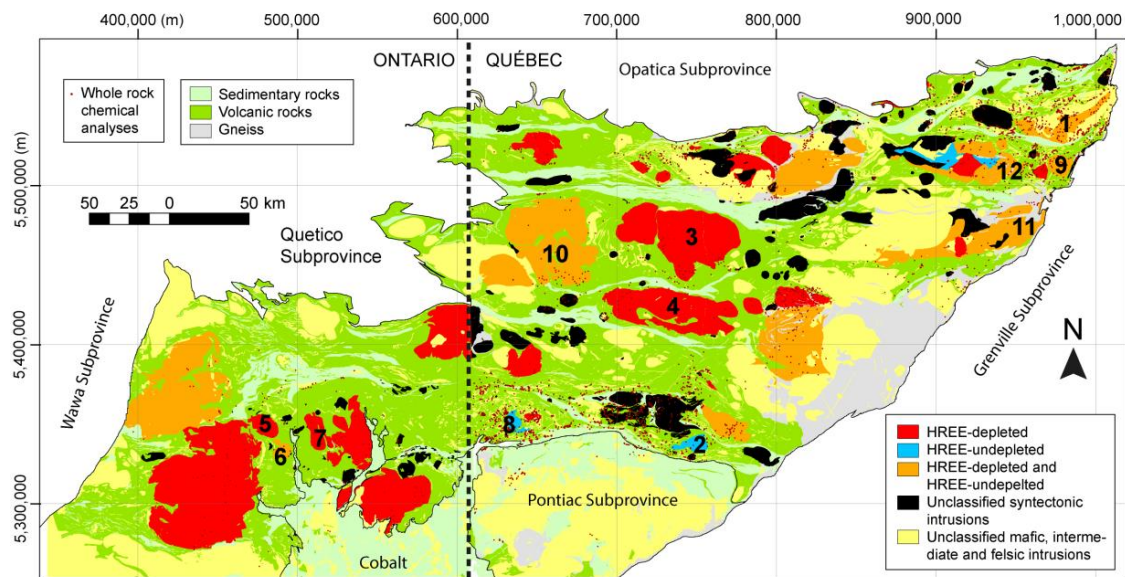


**Figure 7.** Geological map of the Abitibi Subprovince displaying intrusions with strongly fractionated ( $(La/Yb)_N > 6$ ) and less fractionated ( $(La/Yb)_N < 6$ ) REE profiles. Only tonalite, granodiorite, and diorite dominated intrusions are classified. The map is modified from the MERN and OGS datasets, and the projection is UTM NAD83 Zone 17 N. Numbers locate the Chibougamau (1) and Bourlamaque (2) plutons, the Marest (3) and Bernetz (4) batholiths, the Adams (5), Geikie (6) and Blackstock (7) plutons, the Powell, Flavrian, and Dufault plutons (8), La Dauversière (9), Mistouac (10) and Hébert (11) plutons, and the Eau Jaune Complex (12).

Plutons with both HREE-depleted and HREE-undepleted rocks are tonalite and granodiorite, e.g., the Josselin batholith (57 to 75 wt%  $SiO_2$ , median = 71 wt%). Other plutons are more mafic and contain diorite and tonalite, e.g., the Eau Jaune Complex (58 to 75 wt%  $SiO_2$ , median = 65 wt%). In the Hébert, Chibougamau, and Mistouac plutons, HREE-undepleted rocks are diorite and tonalite and HREE-depleted rocks are tonalite and/or granodiorite, whereas in the Josselin batholith and Eau Jaune Complex, diorite, tonalite, and granodiorite are both HREE-depleted and HREE-undepleted. These are synvolcanic intrusions.

## 5. Discussion

The Abitibi Subprovince is a greenstone belt mostly made of volcanic rocks (~40% aerial surface) and intermediate-felsic intrusions (~40%). The remaining 20% is mixed gneisses, metasedimentary rocks, and mafic/ultramafic intrusions. Most of the intermediate-felsic intrusions are classified as tonalite  $\pm$  trondhjemite, and granodiorite (TTG suites). Diorite is a minor lithology; hence, TTD suites only represent ~7–15 % of the intermediate-felsic intrusions (Figure 1). Diorite-rich plutons are, importantly, most abundant in two areas: 1) the north-eastern corner in the Chibougamau area, and 2) in the southern part next to the gold-endowed Cadillac-Larder Lake fault zone (Figure 1).

Synvolcanic and syntectonic intrusions are well distributed in the Abitibi Subprovince, but synvolcanic plutons are most abundant (Figure 2), as in other greenstone belts [2]. The studied intrusions displayed a range of major and trace element compositions and were classified based on their HREE-abundance and  $(La/Yb)_N$  ratio. Intrusions with distinct  $(La/Yb)_N$  ratios were well distributed in the study area and formed during the synvolcanic and syntectonic geodynamic periods. This contribution focuses on two intrusive suites that are dominated by tonalite, granodiorite-granite, and diorite, i.e., on TTG and TTD suites. Whereas most samples are HREE-depleted, as is expected for TTG suites [10], a significant proportion of them (30% for the Sigeom dataset) are HREE-undepleted rocks. These HREE-depleted and HREE-undepleted rocks may correspond to differentiated magmas derived from two main types of primitive magmas.

Rocks characterized by  $(La/Yb)_N > 6$  (Figure 5) display chemical characteristics similar to TTG suites, except that TTG suites are generally more La enriched with  $(La/Yb)_N > 15$  [10]. These HREE-depleted rocks of the Abitibi Subprovince are Na-rich, mostly felsic, and were likely derived from magmas produced by high-pressure melting of hydrated basalt [10]. The source of these magmas is an enriched basalt [9] introduced at depth by a subduction process, delamination, or other processes [3,36,37]. The HREE-depleted rocks of the Abitibi Subprovince also lack a mafic association—mafic enclaves of footwall rocks excepted (not considered here)—and the few intermediate rocks with  $Zr/Ti < 0.01$  may correspond to cumulates (e.g., amphibole-rich area).

According to their Yb content, 75% of the 588 analyzed samples were ‘low HREE-high-pressure TTGs’ defined by  $Yb < 1$  ppm [10]. Other rocks were more Yb enriched (14% with  $1 < Yb < 1.5$  ppm; 5% with  $1.5 < Yb < 2$  ppm; 5% with  $> 2$  ppm Yb) and may have been produced by lower pressure partial melting of hydrated mafic crust [10]. The bulk of HREE-depleted rocks display primitive-mantle normalized negative Ta, Nb, and Ti anomalies likely inherited from the primitive magma, i.e., Ta, Nb, and Ti were retained in the source by a Ti bearing residual phase(s). That their REE contents decrease with increasing  $SiO_2$  suggests a fractional crystallization process controlled by amphibole and, possibly, apatite [38,39]. The Eu anomaly is influenced by the fractionation and accumulation of feldspar and amphibole, which preferentially incorporate  $Eu^{2+}$  and  $Eu^{3+}$ , respectively [40,41]. Hence, significant fractionation of both these minerals may explain the lack of an Eu anomaly (Figure 5a). Amphibole fractionation points to elevated water content and potentially moderate to elevated oxygen fugacity ( $fO_2$ ), as confirmed by a median  $FeO/(FeO + Fe_2O_3)$  ratio of 3.7. The features reported here also characterized other TTG suites [10].

The HREE-depleted rocks were also characterized by a high Sr/Y ratio (Figure 8a). This signature can be achieved through several processes, including deep partial melting with abundant residual garnet and fractional crystallization [42,43]. In the Abitibi Subprovince, this signature likely results from a combination of high-pressure melting of a hydrated basalt source (low Y content) and fractional crystallization (variable Sr content and Sr/Y ratio) (Figure 8a). Besides their Sr content, the HREE-depleted rocks are a chemically diverse group spanning a range of major element content. The major and trace elements content of TTG suites is generally interpreted in terms of depth of partial melting, with the most HREE-depleted and Na-rich magmas produced by higher-pressure melting of the hydrated mafic crust [10]. However, recent studies show that these magmas differentiate significantly upon ascent [39,44]. Thus, the HREE-depleted rocks of the Abitibi Subprovince likely have a homogeneous source, and their noted compositional diversity (e.g., Yb content) is a consequence of lower to upper crustal differentiation—fractional crystallization likely—and is not indicative of a variable depth of partial melting.

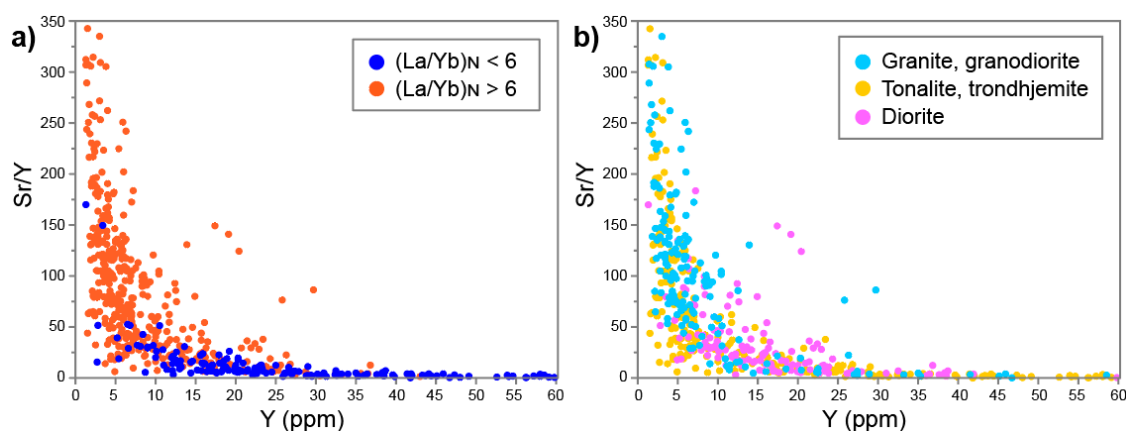


**Figure 8.** Chemistry of intermediate-felsic intrusive rocks of the Sigeom dataset displayed on the Sr/Y vs. Y binary diagram. Only rocks recognized as granite, granodiorite, tonalite, trondhjemite, and diorite in the field, with REE, Y, and Sr analyzed, are displayed ( $n = 558$ ). Color code corresponds to the HREE content (a) and field-based names (b).

In the study area, high-pressure partial melting of hydrated mafic source likely formed HREE-depleted tonalitic magma that subsequently differentiated to form trondhjemite and granodiorite (Figure 8b), as the SiO<sub>2</sub> and K<sub>2</sub>O contents of the melt increased. According to this hypothesis, HREE-depleted rocks with heterogeneous major element chemistry observed in the same batholith may share a common primitive magma and may correspond to the TTG series. Thus, the apparent point alignment of data on TAS and AFM diagrams (Figure 3) may be interpreted as liquid lines of descent, but this hypothesis remains to be tested using dedicated petrogenetic and isotopic studies. A minor amount of the HREE-depleted rocks was identified as diorite, which suggested a possible interaction between the TTG melt and a limited amount of mantle-derived magma.

Rocks characterized by  $(La/Yb)_N < 6$  (Figure 6), in contrast, lack HREE depleted signatures and indicate a garnet-barren source region. These rocks lack primitive-mantle normalized Ta anomalies, and negative Ti and Eu anomalies are only observed in the most felsic rocks. These Ti and Eu anomalies are unlikely to be inherited from a primitive magma and are likely a consequence of fractionation. In contrast, as Nb anomalies are observed in most rocks, this is likely a signature inherited from the primitive magma. The Eu anomaly suggests low to moderate  $fO_2$  conditions that are confirmed by a median FeO/(FeO + Fe<sub>2</sub>O<sub>3</sub>) ratio of 1.2. Differentiation also produced increasing  $\Sigma REEs$  and indicated a limited role for amphibole fractionation. Thus, these suites lacking depleted HREE signatures were related to magmas having lower relative H<sub>2</sub>O contents than the amphibole-rich TTG melts described previously.

The rock characterized by  $(La/Yb)_N < 6$  also displayed chemical variations likely due to differentiation. As differentiation (fractional crystallization in this case) progresses, these magmas are not significantly enriched in iron (Figure 3b), as is also typical for calc-alkaline series in modern-day subduction settings. However, the Archean suites differ from typical calc-alkaline magmas by their absence of K enrichment during differentiation and low LREE-content (Figure 6). On the other hand, the suites characterized by  $(La/Yb)_N < 6$  were LREE enriched compared to evolved tholeiitic rocks such as the soda-granophyre unit (tonalite) observed at the roof of the Lac Dore Complex layered intrusion [21,45]. In summary, the suites lacking HREE depletion had characteristics of both mantle-derived magmas (high HREE content, the abundance of intermediate units, low- to moderate  $fO_2$ , and water content) and TTG melts (Na-rich, LREE enriched, negative Nb anomaly, an abundance of felsic units). These could be mantle-derived melts that hybridized with TTG melts in the lower crust, where mixing of magmas with distinct viscosities was most likely.

This hypothesis was tentatively tested by calculating the trace element content of a mixture of TTG and tholeiitic melts (Figure 9). Median values for the least differentiated HREE-depleted rocks and basalts of the Sigeom dataset were used to approximate the chemistry of primitive TTG and tholeiitic melts, respectively, and to calculate mixed compositions (Figure 9). The chemistry of the SiO<sub>2</sub>-poorest HREE-undepleted rocks was best approximated by a mixture of 80% basalt and 20% HREE-depleted rocks. The model reproduced the slope of the REE profile (Figure 9a) imperfectly, possibly because median values from intrusive and volcanic rocks represented differentiated melt chemistries (parental magmas?), not primitive magmas. Moreover, for this reason, the most compatible elements (Cr and Cu, especially), as well as Ta, were improperly modeled by this simplistic calculation (Figure 9b). The hybrid origin of the HREE-undepleted magmas is a hypothesis that remains to be tested using dedicated petrogenetic studies focused on differentiation processes.

Rocks with HREE-depleted and HREE-undepleted chemistries are coeval and spatially related, i.e., about half of the batholiths of the Abitibi Subprovince are constructed of both rock types. In this greenstone belt, magma production during the synvolcanic period can be summarized as follows:

- Mantle-derived magma (tholeiitic affinity) formed lava flow piles and layered intrusions, and locally induced anatexis to produce felsic magmas emplaced as flows and pyroclastic units with calc-alkaline-like affinities [4];
- High-pressure partial melting of basalt (TTG magma) formed plutons possibly associated with volcanic units [46];



- Hybrid magmas from the mixing of TTG melt and tholeiitic magma formed plutons and, possibly, volcanic units that remain to be identified.

The magma types enumerated above also intruded the upper crust during the syntectonic period, next to additional magma types such as sanukitoid and alkaline intrusions. The magmatic record of the synvolcanic period shows that mantle-derived magmas form a more significant part of tonalite-dominated batholiths than previously recognized. Geodynamic models should account for the specificity of magmatism to evaluate the evolution of the Abitibi Subprovince. By showing that chemical diversity is partially a consequence of differentiation rather than exclusively a function of the depth of partial melting, geodynamic models referring to progressively steeper subduction to explain the HREE content of TTG suites become unreasonable [47,48].

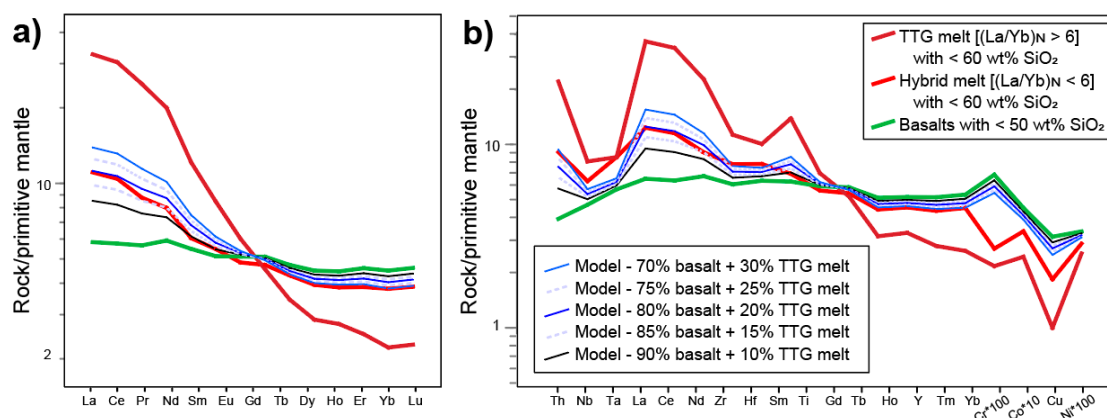


**Figure 9.** Median values displayed on (a) a primitive mantle-normalized [33] REE plot and (b) a primitive-mantle normalized [31] multi-element arachnid diagram modified from Pearce [35]. The median values for the least differentiated (<60 wt% SiO<sub>2</sub>) intermediate-felsic intrusions with (La/Yb)<sub>N</sub> < 6 ( $n = 115$ ) and (La/Yb)<sub>N</sub> > 6 ( $n = 87$ ) are displayed as red lines. Green lines correspond to the least differentiated basalts of the Abitibi Subprovince (Sigeom dataset) with REE, and other trace elements analyzed, and with 45 wt% < SiO<sub>2</sub> < 50 wt% ( $n = 913$ ). Modeled melts (blue and black lines) correspond to a mixture of 70% to 90% basalt (~tholeiitic melt) and 30% to 10% least differentiated HREE-depleted rocks (~TTG melt).

The main synvolcanic magmatic-hydrothermal systems documented in the Abitibi Subprovince are genetically related to TTD suites, i.e., to plutons that may contain hybrid magmas (Chester intrusive complex) or both TTG and hybrid magmas (Chibougamau pluton), according to published REE-profiles [5,6]. These plutons may contain a significant amount of mantle-derived magma, and in both cases, the mineralizing systems have been discussed and compared to porphyry deposits [49]. In modern subduction and post-subduction settings, porphyry mineralized settings require metal-bearing magmas with relatively elevated  $fO_2$  that are emplaced in the upper crust [50–52], and which relate to long-lived magmatic systems [53]. In the Abitibi Subprovince, dedicated studies are required to evaluate these factors better, that is, the emplacement depth of the main batholiths and the duration of magmatic events. Whole-rock chemistry, which indicates limited Eu anomalies and low FeO/[FeO + Fe<sub>2</sub>O<sub>3</sub>] ratios, suggests a favorable  $fO_2$ , but this parameter should be characterized using zircon chemistry. The Cl, S, and metal contents of source rocks (basalt for TTG magma, mantle rock for tholeiites) also remain to be quantified by more detailed studies. However, even with the noted limitations, hybrid magmas may have the best potential to generate Cu-Au magmatic-hydrothermal systems because: 1) mantle-derived magmas may contain more metals than magmas derived from crustal rocks; or 2) hybridization produces magmas with intermediate  $fO_2$  possibly close to one unit above the fayalite-magnetite-quartz solid oxygen buffer (FMQ + 1), which approaches  $fO_2$  conditions for which magma can dissolve the largest amount of gold [54]. Evaluation of petrogenetic models and



physico-chemical parameters should help clarify magmatic-hydrothermal metallogenic models and identify magmas with favorable chemistry that can be targeted by exploration programs.

## 6. Conclusions

Tonalite-dominated magmatism, in the Abitibi Subprovince, derives from two main parental magmas: (1) a TTG melt from high pressure melting of a hydrated basalt source; and (2) a hybrid TTD melt that may be a mixture of mantle-derived magma (tholeiitic melt) and TTG melt. Both magmas significantly differentiated, and the intrusive suites observed in the field may correspond to TTG and TTD magma series. The TTG, on the one hand, are HREE-depleted and are characterized by low HREE, Y, Ti, Nb, and Ta contents (garnet and Ti-mineral bearing source), elevated Sr content and Sr/Y ratio (barren feldspar source), and elevated H<sub>2</sub>O and Na contents (hydrated basalt source). These characteristics, as well as the lack of mafic components, are inherited from the primitive magma ('source signature') and are features that also characterize other TTG suites [10]. This magma crystallized mostly plagioclase and amphibole, as well as quartz, biotite, and K-feldspar, which are the main phases observed in tonalite, trondhjemite, and granodiorite-granite in the field. Differentiation induced an  $\Sigma$ REE decrease, SiO<sub>2</sub> and slight K<sub>2</sub>O enrichment, as well as a limited increase of the K/Na ratio. The rocks derived from hybrid melts, on the other hand, have inherited characteristics of the mantle-derived magma (high HREE content, an abundance of intermediate units, low- to moderate *f*O<sub>2</sub> and water content) and of the TTG melt (Na-rich, LREE enriched, negative Nb anomaly, an abundance of felsic units). Fractional crystallization induced an  $\Sigma$ REE increase, SiO<sub>2</sub> enrichment, as well as negative Eu and Ti anomalies (feldspar and titanite fractionation). Dedicated studies are required to explain their lack of K enrichment during differentiation. Evaluating the implication of these conclusions for porphyry mineralization will require documenting the critical parameters that trigger efficient magmatic-hydrothermal systems. It remains unclear whether mantle or mafic crust is a better source for metals and volatiles, and which source produces magmas with optimal *f*O<sub>2</sub> for gold and base metal transportation in magmatic systems. Additionally, by analogy with modern systems [55], the mingling of magmas with distinct chemistries, in the upper crust, may be essential to mineralizing processes.

**Supplementary Materials:** The following are available online at <http://www.mdpi.com/2075-163X/10/3/242/s1>, Supplementary-material-1.pdf—contains maps, arachnid, and major element diagrams for the intrusions mentioned in the text, Supplementary-material-2.pdf—contains the main phases (aerial extent and proportion) for the intrusions mentioned in the text.

**Author Contributions:** Conceptualization, methodology, writing—original draft preparation, L.M.; writing—review and editing, L.M., D.J.K., and A.C. All authors have read and agreed to the published version of the manuscript.

**Funding:** This study was undertaken as part of the Metal Earth project (Laurentian University) investigation of the Chibougamau area. This research was funded by the Canada First Research Excellence Funds and federal/provincial/industry partners (<http://merc.laurentian.ca/research/metal-earth/>). This project was also funded by the NSERC (Natural Sciences and Engineering Research Council) Discovery Grant to L. Mathieu (Reference number RGPIN-2018-06325).

**Acknowledgments:** Many thanks to three anonymous reviewers who commented on this contribution. Warm thanks are addressed to all the researchers that discussed Archean magmatism with the authors through the years. The authors also addressed thanks to the MERN and OGS for their remarkable dataset. This paper is Metal Earth contribution number MERC-ME-2020-049.

**Conflicts of Interest:** The authors declare no conflict of interest.

## References

1. Goodwin, A.M.; Ridler, R.H. The Abitibi orogenic belt. In Proceedings of the Symposium on basins and geosynclines of the Canadian Shield, Wininipeg, MB, Canada, 10–15 May 1970; Baer, A.J., Ed.; Geological Association of Canada: St. John, NL, Canada, 1970; Volume 70, pp. 1–31.

2. Laurent, O.; Martin, H.; Moyen, J.-F.; Doucelance, R. The diversity and evolution of late-Archean granitoids: Evidence for the onset of “modern-style” plate tectonics between 3.0 and 2.5 Ga. *Lithos* **2014**, *205*, 208–235. [[CrossRef](#)]
3. Moyen, J.-F.; Laurent, O. Archean tectonic systems: A view from igneous rocks. *Lithos* **2018**, *302*, 99–125. [[CrossRef](#)]
4. Mathieu, L.; Snyder, D.B.; Bedeaux, P.; Cheraghi, S.; Lafrance, B.; Thurston, P.; Sherlock, R. Deep into the Chibougamau area, Abitibi Subprovince: structure of a Neoproterozoic crust revealed by seismic reflection profiling. *Earth Sp. Sci. Open Arch.* **2020**. [[CrossRef](#)]
5. Katz, L.R.; Kontak, D.J.; Dubé, B.; McNicoll, V. The geology, petrology, and geochronology of the Archean Côté Gold large-tonnage, low-grade intrusion-related Au ( $\pm$ Cu) deposit, Swayze greenstone belt, Ontario, Canada. *Can. J. Earth Sci.* **2017**, *54*, 173–202. [[CrossRef](#)]
6. Mathieu, L.; Racicot, D. Petrogenetic Study of the Multiphase Chibougamau Pluton: Archean Magmas Associated with Cu-Au Magmato-Hydrothermal Systems. *Minerals* **2019**, *9*, 174. [[CrossRef](#)]
7. Leclerc, F.; Roy, P.; Pilote, P.; Bédard, J.H.; Harris, L.B.; McNicoll, V.J.; van Breemen, O.; David, J.; Goulet, N. *Géologie de la Région de Chibougamau*; MERN report RG 2015-03; Ministère de l'Énergie et des Ressources Naturelles: Québec, QC, Canada, 2017.
8. Thurston, P.C.; Ayer, J.A.; Goutier, J.; Hamilton, M.A. Depositional gaps in Abitibi greenstone belt stratigraphy: A key to exploration for syngenetic mineralization. *Econ. Geol.* **2008**, *103*, 1097–1134. [[CrossRef](#)]
9. Martin, H.; Moyen, J.-F.; Guitreau, M.; Blichert-Toft, J.; Le Pennec, J.-L. Why Archean TTG cannot be generated by MORB melting in subduction zones. *Lithos* **2014**, *198*, 1–13. [[CrossRef](#)]
10. Moyen, J.-F.; Martin, H. Forty years of TTG research. *Lithos* **2012**, *148*, 312–336. [[CrossRef](#)]
11. SIGEOM Système d'information géominière du Québec. Available online: <http://sigeom.mines.gouv.qc.ca> (accessed on 1 January 2020).
12. Montsion, R.M.; Thurston, P.; Ayer, J. Superior Data Compilation. Available online: <https://merc.laurentian.ca/research/metal-earth/superior-compilation> (accessed on 1 January 2020).
13. Beakhouse, G.P. *The Abitibi Subprovince Plutonic Record: Tectonic and Metallogenic Implications*; Open File report 6268; Ontario Geological Survey: Sudbury, ON, Canada, 2011.
14. Carr, S.D.; Easton, R.M.; Jamieson, R.A.; Culshaw, N.G. Geologic transect across the Grenville orogen of Ontario and New York. *Can. J. Earth Sci.* **2000**, *37*, 193–216. [[CrossRef](#)]
15. Percival, J.A.; West, G.F. The Kapuskasing uplift: a geological and geophysical synthesis. *Can. J. Earth Sci.* **1994**, *31*, 1256–1286. [[CrossRef](#)]
16. Mortensen, J.K. U-Pb geochronology of the eastern Abitibi subprovince. Part 1: Chibougamau–Matagami–Joutel region. *Can. J. Earth Sci.* **1993**, *30*, 11–28. [[CrossRef](#)]
17. Krogh, T.E. Improved accuracy of U-Pb zircon ages by the creation of more concordant systems using an air abrasion technique. *Geochim. Cosmochim. Acta* **1982**, *46*, 637–649. [[CrossRef](#)]
18. Pilote, P.; Dion, C.; Joannise, A.; David, J.; Machado, N.; Kirkham, R.V.; Robert, F. Géochronologie des minéralisations d'affiliation magmatique de l'Abitibi, secteurs Chibougamau et de Troilus-Frotet: implications géotectoniques. In *Programme et résumés, Séminaire d'information sur la recherche géologique*; MRN report, DV-97-03; Ministère des Ressources Naturelles: Québec, QC, Canada, 1997; p. 47.
19. McNicoll, V.; Dubé, B.; Goutier, J.; Mercier-Langevin, P.; Dion, C.; Monecke, T.; Ross, P.-S.; Thurston, P.; Pilote, P.; Bédard, J.; et al. *Nouvelles datations U-Pb dans le Cadre du Projet ICG-3 Abitibi/Plan Cuivre: Incidences pour l'Interprétation Géologique et l'Exploration des Métaux Usuels*; MRN report DV-2008-06; Ministère des Ressources Naturelles: Québec, QC, Canada, 2008.
20. David, J.; Vaillancourt, D.; Bandyayera, D.; Simard, M.; Goutier, J.; Pilote, P.; Dion, C.; Barbe, P. *Datations U-Pb Effectuées dans les Sousprovinces d'Ashuanipi, de La Grande, d'Opinaca et d'Abitibi en 2008–2009*; MERN report, RP-2010-11; Ministère de l'Énergie et des Ressources Naturelles: Québec, QC, Canada, 2011.
21. Allard, G.O. *Doré Lake Complex and its importance to Chibougamau Geology and Metallogeny*; MRN report DPV-386; Ministère des Ressources Naturelles: Québec, QC, Canada, 1976.
22. Mathieu, L. Origin of the Vanadiferous Serpentine-Magnetite Rocks of the Mt. Sorcerer Area, Lac Doré Layered Intrusion, Chibougamau, Québec. *Geosciences* **2019**, *9*, 110. [[CrossRef](#)]
23. Maier, W.D.; Barnes, S.-J.; Pellet, T. The economic significance of the Bell River complex, Abitibi subprovince, Quebec. *Can. J. Earth Sci.* **1996**, *33*, 967–980. [[CrossRef](#)]

24. Paradis, S.; Ludden, J.; Gélinas, L. Evidence for contrasting compositional spectra in comagmatic intrusive and extrusive rocks of the late Archean Blake River Group, Abitibi, Quebec. *Can. J. Earth Sci.* **1988**, *25*, 134–144. [[CrossRef](#)]
25. Feng, R.; Kerrich, R. Single zircon age constraints on the tectonic juxtaposition of the Archean Abitibi greenstone belt and Pontiac subprovince, Quebec, Canada. *Geochim. Cosmochim. Acta* **1991**, *55*, 3437–3441. [[CrossRef](#)]
26. Middlemost, E.A.K. Naming materials in the magma/igneous rock system. *Earth-Science Rev.* **1994**, *37*, 215–224. [[CrossRef](#)]
27. Irvine, T.N.J.; Baragar, W. A guide to the chemical classification of the common volcanic rocks. *Can. J. Earth Sci.* **1971**, *8*, 523–548. [[CrossRef](#)]
28. Winchester, J.A.; Floyd, P.A. Geochemical discrimination of different magma series and their differentiation products using immobile elements. *Chem. Geol.* **1977**, *20*, 325–343. [[CrossRef](#)]
29. Streckeisen, A. Classification and nomenclature of volcanic rocks, lamprophyres, carbonatites, and melilitic rocks: Recommendations and suggestions of the IUGS Subcommittee on the Systematics of Igneous Rocks. *Geology* **1979**, *7*, 331–335. [[CrossRef](#)]
30. Le Maitre, R.W.; Streckeisen, A.; Zanettin, B.; Le Bas, M.J.; Bonin, B.; Bateman, P.; Bellieni, G.; Dudek, A.; Efremova, S.; Keller, J. Igneous rocks: A classification and glossary of terms; Recommendations of the International Union of Geological Sciences. In *Subcommission on the Systematics of Igneous Rocks*; Cambridge University Press: Cambridge, UK, 2002; p. 230.
31. Hutchison, C.S. The norm; its variations, their calculation and relationships. *Schweizerische Mineral. und Petrogr. Mitteilungen* **1975**, *55*, 243–256.
32. Le Maitre, R.W. The chemical variability of some common igneous rocks. *J. Petrol.* **1976**, *17*, 589–598. [[CrossRef](#)]
33. Hofmann, A.W. Chemical differentiation of the Earth: the relationship between mantle, continental crust, and oceanic crust. *Earth Planet. Sci. Lett.* **1988**, *90*, 297–314. [[CrossRef](#)]
34. McDonough, W.F.; Sun, S.-S. The composition of the Earth. *Chem. Geol.* **1995**, *120*, 223–253. [[CrossRef](#)]
35. Pearce, J.A. Geochemical fingerprinting of oceanic basalts with applications to ophiolite classification and the search for Archean oceanic crust. *Lithos* **2008**, *100*, 14–48. [[CrossRef](#)]
36. Kerrich, R.; Polat, A. Archean greenstone-tonalite duality: thermochemical mantle convection models or plate tectonics in the early Earth global dynamics? *Tectonophysics* **2006**, *415*, 141–165. [[CrossRef](#)]
37. Bedard, J.H.; Harris, L.B.; Thurston, P.C. The hunting of the snArc. *Precambrian Res.* **2013**, *229*, 20–48. [[CrossRef](#)]
38. Hanson, G.N. The application of trace elements to the petrogenesis of igneous rocks of granitic composition. *Earth Planet. Sci. Lett.* **1978**, *38*, 26–43. [[CrossRef](#)]
39. Liou, P.; Guo, J. Generation of Archean TTG Gneisses Through Amphibole Dominated Fractionation. *J. Geophys. Res. Solid Earth* **2019**, *124*, 3605–3619. [[CrossRef](#)]
40. Klein, M.; Stosch, H.-G.; Seck, H.A. Partitioning of high field-strength and rare-earth elements between amphibole and quartz-dioritic to tonalitic melts: an experimental study. *Chem. Geol.* **1997**, *138*, 257–271. [[CrossRef](#)]
41. Drake, M.J.; Weill, D.F. Partition of Sr, Ba, Ca, Y, Eu<sup>2+</sup>, Eu<sup>3+</sup>, and other REE between plagioclase feldspar and magmatic liquid: an experimental study. *Geochim. Cosmochim. Acta* **1975**, *39*, 689–712. [[CrossRef](#)]
42. Moyen, J.-F. High Sr/Y and La/Yb ratios: the meaning of the “adakitic signature”. *Lithos* **2009**, *112*, 556–574. [[CrossRef](#)]
43. Richards, J.P.; Kerrich, R. Special paper: adakite-like rocks: their diverse origins and questionable role in metallogenesis. *Econ. Geol.* **2007**, *102*, 537–576. [[CrossRef](#)]
44. Laurent, O.; Björnsen, J.; Wotzlaw, J.-F.; Bretscher, S.; Silva, M.P.; Moyen, J.-F.; Ulmer, P.; Bachmann, O. Earth’s earliest granitoids are crystal-rich magma reservoirs tapped by silicic eruptions. *Nat. Geosci.* **2020**, 1–7. [[CrossRef](#)]
45. Allard, G.O.; Caty, J.L. *Géologie du quart nord-est et d’une partie du quart sud-est du canton de Lemoine, comtés d’Abitibi-Est et de Roberval*; MRN report RP-566; Ministère des ressources naturelles: Québec, QC, Canada, 1969.
46. Gaboury, D. Geochemical approaches in the discrimination of synvolcanic intrusions as a guide for volcanogenic base metal exploration: an example from the Abitibi belt, Canada. *Appl. Earth Sci.* **2006**, *115*, 71–79. [[CrossRef](#)]

47. Abbott, D.; Drury, R.; Smith, W.H.F. Flat to steep transition in subduction style. *Geology* **1994**, *22*, 937–940. [[CrossRef](#)]
48. Martin, H.; Moyen, J.-F. Secular changes in tonalite-trondhjemite-granodiorite composition as markers of the progressive cooling of Earth. *Geology* **2002**, *30*, 319–322. [[CrossRef](#)]
49. Pilote, P. *Metallogenic Evolution and Geology of the Chibougamau Area—from Porphyry Cu-Au-Mo to Mesothermal Lode Gold Deposits*; Open File 3143; Geological Survey of Canada: Québec, QC, Canada, 1995.
50. Sillitoe, R.H. Porphyry copper systems. *Econ. Geol.* **2010**, *105*, 3–41. [[CrossRef](#)]
51. Richards, J.P. Postsubduction porphyry Cu-Au and epithermal Au deposits: Products of remelting of subduction-modified lithosphere. *Geology* **2009**, *37*, 247–250. [[CrossRef](#)]
52. Richards, J.P. A shake-up in the porphyry world? *Econ. Geol.* **2018**, *113*, 1225–1233. [[CrossRef](#)]
53. Chiaradia, M.; Caricchi, L. Stochastic modelling of deep magmatic controls on porphyry copper deposit endowment. *Sci. Rep.* **2017**, *7*, 1–11. [[CrossRef](#)] [[PubMed](#)]
54. Botcharnikov, R.E.; Linnen, R.L.; Wilke, M.; Holtz, F.; Jugo, P.J.; Berndt, J. High gold concentrations in sulphide-bearing magma under oxidizing conditions. *Nat. Geosci.* **2011**, *4*, 112. [[CrossRef](#)]
55. Chelle-Michou, C.; Chiaradia, M. Amphibole and apatite insights into the evolution and mass balance of Cl and S in magmas associated with porphyry copper deposits. *Contrib. to Mineral. Petrol.* **2017**, *172*, 105. [[CrossRef](#)]



© 2020 by the authors. Licensee MDPI, Basel, Switzerland. This article is an open access article distributed under the terms and conditions of the Creative Commons Attribution (CC BY) license (<http://creativecommons.org/licenses/by/4.0/>).